

The polymorphic behaviour of poly(2,2-dimethyltrimethylenecarbonate) and of its cyclic monomer. Evidence for a high entropy, conformationally disordered modification

Giancarlo Sidoti^a, Silvia Capelli^a, Stefano V. Meille^{a,*} and Giovanni C. Alfonso^b

^a*Dipartimento di Chimica, Politecnico di Milano, via Mancinelli 7, 20131 Milano, Italy*

^b*Dipartimento di Chimica e Chimica Industriale, Università di Genova,*

Via Dodecaneso 31, 16146 Genova, Italy

(Received 15 October 1996; revised 19 December 1996)

Poly(2,2-dimethyltrimethylenecarbonate) (PDTC) and its cyclic monomer 5,5-dimethyl-1,3-dioxan-2-one (DTC) are characterised by X-ray diffraction, calorimetry, dilatometry and conformational energy calculations. Three crystalline modifications are identified for PDTC: form I from solution, form III in melt spun fibers, while form II, obtained from the melt at surprisingly small undercoolings shows unusually large coherent domain dimensions, chain extended morphology and a modest enthalpy of fusion. These features indicate that form II should be a high entropy, conformationally disordered phase. Conformational calculations identify four regular, extended conformations with similar low energy, which are consistent with the observed polymorphic behaviour of PDTC. The cyclic monomer DTC also shows three crystalline modifications: a low temperature, ordered form and two high temperature phases, which like the polymer, are characterised by high entropy presumably due to conformational and orientational disorder. © 1997 Elsevier Science Ltd.

(Keywords: polycarbonates; polymorphism; X-ray diffraction)

INTRODUCTION

Aliphatic polycarbonates attract increasing interest as hydrolytically and thermally degradable polymers. Poly(2,2-dimethyltrimethylenecarbonate) [PDTC, see Figure 1(a)] and its copolymers were tested for biomedical applications¹ and were found to be biocompatible. These systems are also under consideration in biodegradable random-copolymers for the production of low environmental impact materials.

Investigations published so far mainly dealt with the synthesis of PDTC by anionic ring-opening polymerisation^{2,3} of 5,5-dimethyl-1,3-dioxan-2-one [DTC, see Figure 1(b)], while the available physico-chemical data are scarce.

The present paper reports the thermal, structural and conformational characterisation of the polymorphic behaviour of PDTC by differential scanning calorimetry, dilatometry and X-ray diffraction. Three different crystalline phases were identified: form I crystallises from solution, form II is obtained from the melt and a third modification develops in melt spun fibers. Conformational calculations were also carried out to help rationalise this complex behaviour. DSC, dilatometric and X-ray diffraction (single crystal and powder) data are discussed also for the cyclic monomer because of their relevance to the behaviour of the polymer. It is noteworthy that DTC also exhibits polymorphism with substantial analogies to the polymer.

EXPERIMENTAL

Three samples with different molecular weight were used: PDTC2 ($M_w = 20\,000$), PDTC5 ($M_w = 50\,000$) and PDTC7 ($M_w = 70\,000$). Both PDTC2 and PDTC5 samples contain a central bifunctional block of triethylenoxide ($-O-CH_2-CH_2-$)₃ used as initiator. 'Native' samples were obtained by precipitation of toluene solutions with methanol to remove the oligomers. ¹³C NMR spectra (250 MHz) of PDTC2, PDTC7 and DTC were recorded in CDCl₃. The chemical shifts were determined with respect to TMS internal standard. The ¹³C NMR spectra show respectively four singlets at δ 20.99 (CH₃), δ 28.38 (C), δ 77.49 (CH₂), δ 149.24 (C=O) ppm for DTC and four singlets at δ 21.38 (CH₃), δ 35.11 (C), δ 72.40 (CH₂), δ 155.30 (C=O) ppm for the polymers (PDTC2 and PDTC7). Unassigned resonances suggest that impurities are well below 5%; the spectra do not change after the samples are subjected to typical thermal treatments (see below).

The calorimetric studies were carried out using a Perkin Elmer DSC7 system equipped with a CCA7 liquid nitrogen cooling device. Samples were heated from -50 to 150°C (first heating cycle), immediately cooled to -50°C and heated again to 150°C (second heating cycle). The typical heating and cooling rates were $10^\circ\text{C}/\text{min}$. For the DTC sample the DSC curves were recorded between 20°C and 150°C .

The dilatometric curves (specific volume *versus* temperature), for PDTC2 films cast at room temperature from a solution of CH₂Cl₂ and for DTC were recorded at $10^\circ\text{C}/\text{hr}$ from 25 to 145°C and 130°C , respectively.

X-ray diffraction spectra were recorded both from unoriented (form I and II) and oriented samples (form II

* To whom correspondence should be addressed

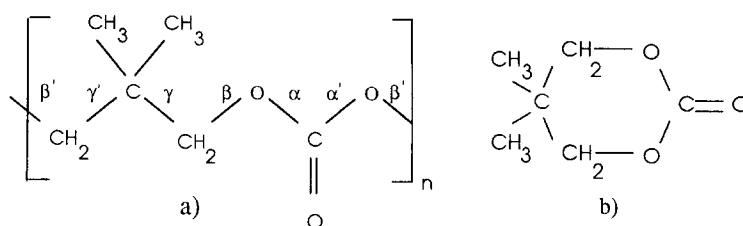


Figure 1 (a) The PDTC repeat unit identifying the torsion angles discussed in the text; and (b) the DTC monomer.

and fibers) of PDTC. Partially oriented PDTC7 form II samples were obtained by shearing the undercooled melt while good fibers resulted by additional stretching at room temperature of melt spun fibers. Unoriented samples were studied in a θ/θ Italstructures diffractometer, while sheared samples and fibers were studied both with cylindrical and Kiessig vacuum cameras. The former had a radius of 57.3 mm and in the latter a film-sample distance of about 100 mm was adopted. The same Kiessig camera with film-sample distances of 400 mm and 500 mm was used for small angle X-ray diffraction (SAXS) measurements. Ni-filtered Cu- $K\alpha$ radiation was used throughout.

X-ray diffraction data of a colorless crystal of DTC ($1.3 \times 0.4 \times 0.2$ mm) were collected on a Siemens P4 diffractometer, with graphite monochromated Cu- $K\alpha$ radiation ($\lambda = 1.5418$ Å). The DTC crystal was enclosed in a glass capillary for roentgenographic uses because of its low sublimation temperature.

Crystal data for DTC: $M = 130.14$, monoclinic, space group $P2_1/n$, $a = 14.533(1)$, $b = 6.508(1)$, $c = 14.508(2)$, $\beta = 92.60(1)$, $V = 1370.7(3)$ Å³, $Z = 8$, $D_{\text{calc}} = 1.261$ g/cm³, $D_{\text{exp}} = 1.238$ g/cm³ (dilatometric), $F(000) = 560$, $\mu(\text{Cu}-K\alpha) = 0.85$ mm⁻¹.

Lattice constants were determined by least square refinement on 2θ values of 15 reflections with $2\theta > 40^\circ$. Four octants of intensity data (4268 total reflections) were collected using the $\theta/2\theta$ scan technique in the range $2^\circ < 2\theta < 116^\circ$ for 1860 independent reflections ($R_{\text{int}} = 0.0205$). Three standard reflections were monitored every 97 reflections to check crystal orientation and stability. Data were corrected for Lorentz and polarisation effects but no absorption correction was applied.

The crystal structure was solved by direct methods using SIR92⁴ and refined by full-matrix least squares on F^2 values using SHELXL93.⁵ Non-hydrogen atoms were refined with anisotropic temperature factors while hydrogen atoms were refined isotropically. Final values of the residuals R and $wR2$ [for 1606 reflection with $I > 2.0 \sigma(I)$] were 0.0472 and 0.1315, respectively, while Rw for all reflections was 0.0545. The highest and lowest peaks in the final difference Fourier map were 0.197 and -0.242 eÅ⁻³. Final positional parameters and temperature factors have been deposited with the Cambridge Structural Data Service.

The conformational energy calculations were carried out with the CVFF⁶ force field as supplied by Biosym⁷ and with the MM2 force field as in the MACROMODEL⁸ package. Very similar results were obtained with both force fields but for brevity only the values determined with MM2 will be reported. No geometric or symmetry constraints were imposed on the systems. Terminal group effects were cancelled out by minimising the potential energy of chain fragments containing different numbers of monomeric units (between 4 and 12) and comparing results. Calculated energies are given in kJ per mole of monomeric unit. They are averages obtained by subtracting from the minimised

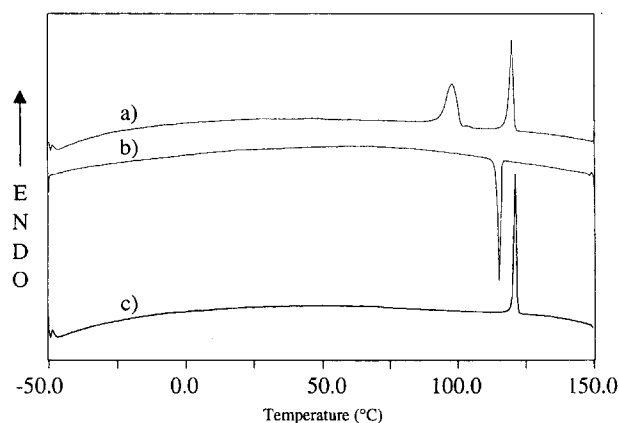


Figure 2 DSC curves for PDTC7 samples: (a) first heating; (b) cooling; and (c) second heating

energy value the terminal group contributions and dividing by the number of monomeric units in the specific oligomer. Also the reported torsion angles were obtained by averaging over the values determined from the four innermost monomeric units in the dodecamer and estimates of the corresponding repeat distances and chain symmetry are the result of a similar procedure. All the calculations have been carried out on a Silicon Graphics Personal Iris 4D.

RESULTS AND DISCUSSION

DSC and X-ray diffraction of PDTC

Consistent with the detailed study of Lebedev *et al.*⁹, differential scanning calorimetry (DSC) investigations of native PDTC7 (Figure 2) show two well defined endotherms at 98°C ($\Delta H \approx 27$ J/g) and at 120°C ($\Delta H \approx 22$ J/g) which correspond respectively to the transition from form I to form II and to isotropisation. This assignment is supported by the X-ray diffraction studies which will be discussed subsequently: we anticipate that no traces of form II can be detected by this technique in samples obtained from solution. During cooling a single exothermic peak at 115°C ($\Delta H \approx 23$ J/g) is observed corresponding to a crystallisation process at a surprisingly small undercooling (5°C). In the second heating only an endothermic peak at 121°C ($\Delta H = 26$ J/g), due to the melting of form II, appears.

The thermal behaviour of PDTC samples of different molecular weights is qualitatively similar. As shown in Table 1, the melting point of form I increases with molecular weight, while the melting enthalpy somewhat surprisingly apparently decreases. The enthalpy differences in the 100°C endotherm could be attributed to a lower degree of crystallinity of high molecular weight solution-crystallised samples but it seems more likely that the effect is mainly related to recrystallisation into form II, because the enthalpy of the 100°C transition is probably the balance

Table 1 Thermal behavior of PDTC samples of different molecular weights

Sample	First Heating				Cooling		Second Heating		
	T_{f1} (°C)	ΔH_{f1} (J/g)	T_{f2} (°C)	ΔH_{f2} (J/g)	T_{c2} (°C)	ΔH_{c2} (J/g)	T_{f2} (°C)	ΔH_{f2} (J/g)	
PDTC2 ^a	95.4	40	108.7	18	91.7	−20	107.7	21	
PDTC5 ^b	95.0	30	113.8	22	104.8	−24	114.8	24	
PDTC7 ^c	97.8	27	119.7	22	115.0	−23	120.8	25	

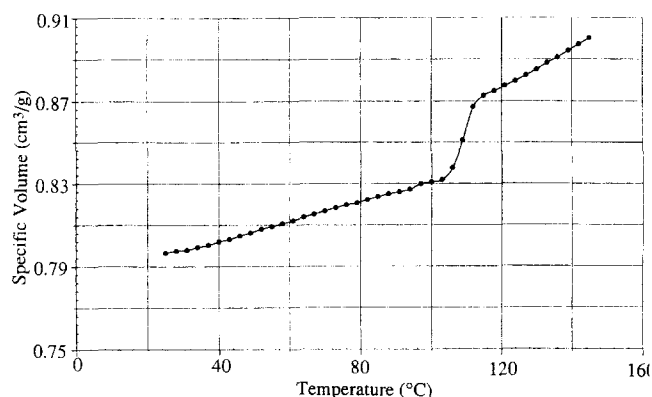
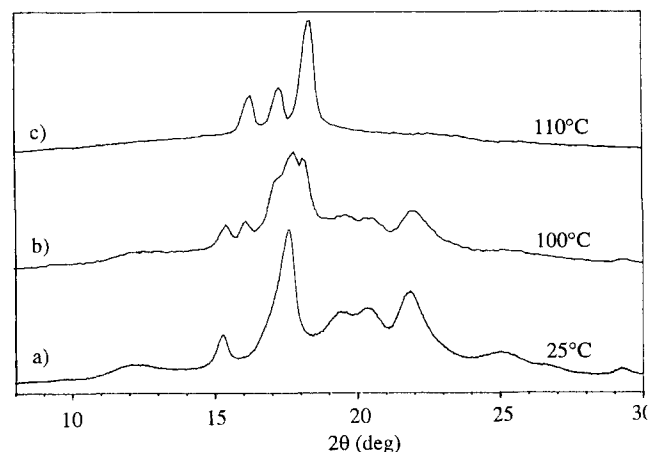
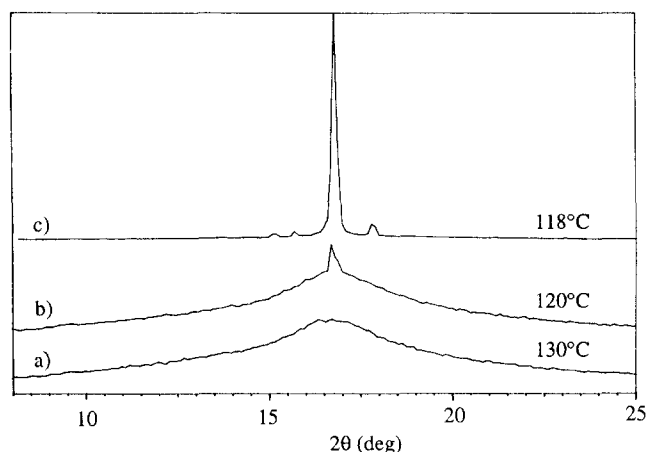
^a $M_w = 20\,000$; ^b $M_w = 50\,000$; ^c $M_w = 70\,000$.

Figure 3 Dilatometric curve for solvent cast PDTC2

Table 2 Measured X-ray diffraction reflections

Form I		Form II	
2θ	\AA	2θ	\AA
10.00	8.83	16.0	5.53
12.24	7.22	17.0	5.21
15.44	5.73	18.2	4.87
17.72	5.00	19.4	4.57
19.56	4.53	21.4	4.15
20.48	4.33	23.5	3.78
21.88	4.06		
25.00	3.56		
26.52	3.36		
29.40	3.03		
30.64	2.91		
34.04	2.66		
37.96	2.37		


Figure 4 X-ray diffraction patterns of native PDTC7 recorded successively at increasing temperatures: (a) 25°C (form I); (b) 100°C (forms I and II); and (c) 110°C (form II)

Figure 5 PDTC7 form II X-ray diffraction patterns recorded at different temperatures on cooling from the melt

between melting of form I and recrystallisation into form II. Table 1 indeed shows that the enthalpy associated with both the melting of form II and its recrystallisation in successive cooling cycles grows with molecular weight while a similar increase is observed also for its melting temperature. The crystallisation rate of form II from the melt also increases with molecular mass as indicated by the lower undercooling at which the exotherm is observed for PDTC7 (Table 1). Furthermore for all samples the enthalpy of fusion of form II in the successive heating scans is clearly higher than in the first, while melting temperatures vary only slightly. Dilatometric results for PDTC2 (Figure 3) are consistent with the DSC data and show two transitions: the first one at low temperature (*ca.* 95°C) with a small volume change, and the second at a higher temperature (*ca.* 110°C) corresponding to the isotropisation of form II.

Figure 4 shows X-ray diffraction patterns of PDTC7 recorded at different temperatures: while the data at 25°C and 110°C as we already noted are clearly due to different crystalline modifications (i.e. respectively form I and form II; see Table 2), the pattern recorded at 100°C shows simultaneous presence of the two forms. We can conclude that while form II is initially absent in solution crystallised samples, it develops as soon as form I melts at approximately 100°C. As we anticipated the endotherm at this temperature represents therefore the enthalpic balance of the two processes. Alternatively, the transition at 100°C could be interpreted as a form I-form II solid–solid transformation, but this is less likely considering the previously discussed effect of molecular weight on the enthalpy associated with the transition and some morphological evidence on solution crystallised crystals obtained from

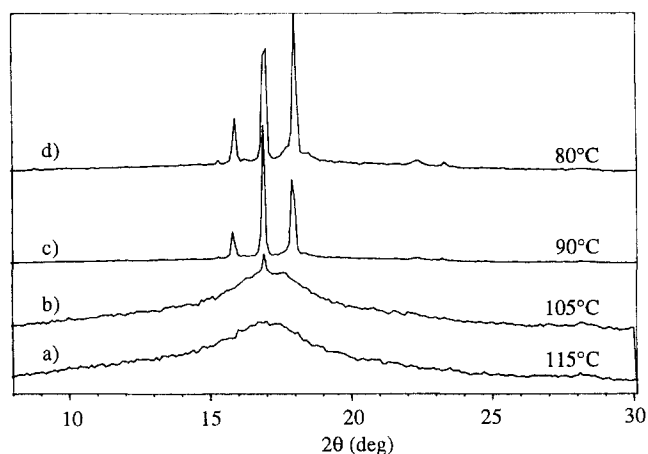


Figure 6 PDTC2 form II X-ray diffraction patterns recorded at different temperatures on cooling from the melt

an electron microscopy investigation to be discussed elsewhere. After complete melting (140°C) we recorded patterns on cooling at different temperatures (Figure 5). At 120°C we can see the development of initial phase II crystallinity as evidenced by the peak at $2\theta = 17.0^\circ$. At 118°C PDTC7 is already highly crystalline and spectra remain essentially unaltered down to room temperature. These features and the substantially higher enthalpy involved in the lower temperature transition as compared to the melting of form II suggest that this last phase could be mesomorphic in nature.

While PDTC2 and PDTC7 behave similarly in the first heating, upon cooling (Figure 6) the X-ray patterns become quite different. The peak at $2\theta = 17.0^\circ$ (90°C) in PDTC2 is relatively less intense than the same peak of PDTC7. Moreover, in the case of PDTC2, the intensity of this peak decreases in the cooling process until, at 80°C, it is not dominant anymore in diffraction patterns. We can suggest that PDTC2 form II crystallises in a different way due to the lower molecular weight. The effect could either be of kinetic nature or be related to morphological features like domain size, etc. while further polymorphism may also play a role.

The full widths at half maximum (FWHM) for both PDTC2 and PDTC7 specimen diffraction maxima have a similar behaviour for the different phases. Form I samples of both polymers present a FWHM of *ca.* 1° for the peak at $2\theta = 17.7^\circ$; form II samples at 25°C, after cooling from 120°C, have a FWHM of *ca.* 0.5° for the peak at $2\theta = 18.2^\circ$ while in specimens recrystallised after complete isotropisation at 140°C the value of FWHM is reduced to *ca.* 0.2° . Other peaks exhibit a similar behaviour. Evidently the coherent domain dimensions increase dramatically from phase I to phase II and apparently further grow upon recrystallisation from the melt. This behaviour is consistent with the small increase of the values of form II enthalpy of fusion in the second heating cycle. The long spacing of PDTC7 form I measured by SAXS is about 65 Å, in good agreement with a TEM value of 60 Å for the thickness of solution crystallised lamellar crystals. After recrystallisation from the melt we were unable to observe SAXS long spacings. Considering the limitations of the experimental apparatus, the lamellar thickness should therefore exceed 300 Å. Thus our data suggest that considerable chain extension occurs in form II samples, hardly changing upon recrystallisation from the melt. In this respect it is interesting to recall that while the 'chain-folded' form I crystals of all the studied samples

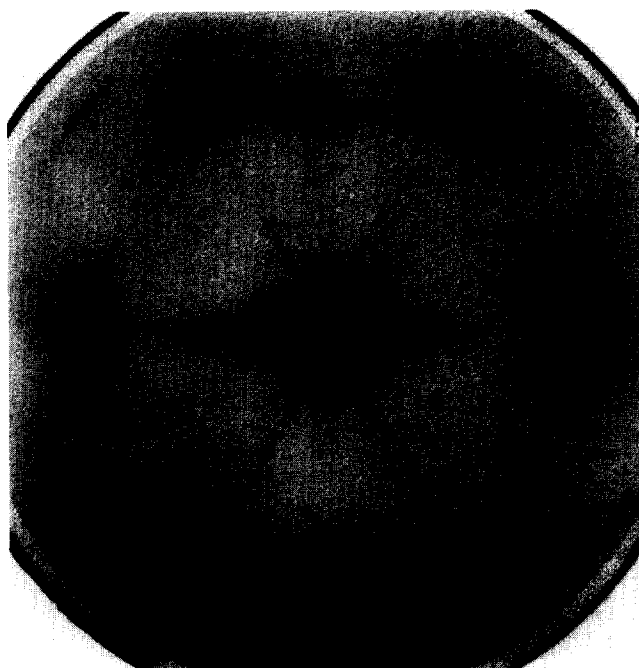


Figure 7 X-ray diffraction pattern of PDTC7 form II obtained from a melt-sheared film (sample edge perpendicular to the beam). The horizontal, i.e. the equator of the pattern, is perpendicular to polymer film surface

show a similar melting temperature, the melting point, and also the melting enthalpies, of the highly 'chain extended' form II crystals increase considerably with molecular weight. The behaviour of form II is indeed similar to that of conformationally disordered mesophases¹⁰ typical of polyphosphazenes and polysiloxanes.

Figure 7 shows the diffraction pattern (sample edge perpendicular to the beam) of PDTC7 form II obtained from melt sheared films. The orientation obtained in the process is typical for a polymeric material. We can notice peaks on the equatorial line at 17.0° (2θ) and on the first layer line at 16.0, 18.2 and 23.5° . The layer line spacing indicates a periodicity of about 5.6 Å or a multiple of this value, which does not need to coincide with the chain repeat. These spectra show extremely sharp, point like diffraction spots, highly unusual for a polymer and confirm that coherent domains have to be very large. This feature is again indicative of the mesomorphic nature of PDTC7 crystallised from the melt. ¹³C NMR solution data allow us to unambiguously exclude the presence of low molecular weight components like monomer or other cyclic oligomers.

We finally report that the melt-spun fibers, when additionally stretched at room temperature, give X-ray diffraction patterns showing a fiber repeat of 7 Å. The observed reflections do not correspond to either form I or II and indicate a still different modification that will be discussed in detail elsewhere.

Conformational analysis of PDTC

Examination of model compounds and of related polyesters like poly(pivalolactone)¹¹, poly(-hydroxybutyrate)¹², polycarbonate¹³, etc. suggests that while for both the α and β torsion angles [Figure 1(a)] the *trans* conformation is clearly favoured, for the γ angle *gauche* conformations should be slightly preferred over *trans*. Furthermore we decided to exclude from the detailed analysis the combinations of opposite *gauche* conformers ($-g^+g^-$) of adjacent $\gamma\gamma'$ angles, because of the obviously high energy of these arrangements.

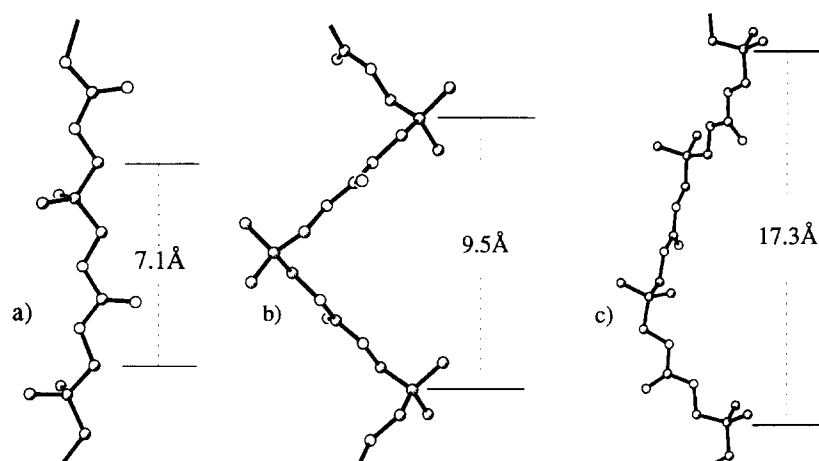


Figure 8 Three low energy conformations of PDTC: (a) all *trans* conformation; (b) 2_1 helix; and (c) 3_1 helix respectively with *gauche*–*gauche* and *gauche*–*trans* γ , γ' torsion angles

At first our investigation was confined to helical conformers respecting the equivalence postulate¹⁴ between successive chemical repeats. Under these assumptions conformational calculations show three low energy conformers. The first [Figure 8(a)] adopts an all-*trans* conformation and displays a repeat fiber period of 7.1 Å with only translational symmetry. Its conformational energy is 3.4 kJ/mole higher than the more stable conformation [Figure 8(b)] which has again all *trans* torsion angles, except for the two γ angles adjacent to the quaternary carbon, which are both *gauche* ($-g^+g^-$). The fiber repeat of this kinked 2_1 helical conformer is 9.5 Å and it has an axial advance per monomer unit that is only 67% of the value of the all *trans* form. The last helical conformation so far identified is of intermediate energy i.e. 0.9 kJ/mole higher than the more stable conformation. It has the two angles near the quaternary carbon respectively *trans* and *gauche* ($-tg^-$) and shows a fiber repeat period of 17.3 Å with 3_1 screw symmetry [Figure 8(c)]. Thus the axial projection per monomer unit for this conformer is 81% of the fully extended conformation.

Because in all the discussed conformations successive $\gamma\gamma'$ pairs are separated by four *trans* bonds, they are in principle hardly correlated. As a consequence, since the regular $(-g^+g^+-tttt)_n$ is a low energy conformation also the $(-g^+g^+-tttt-g^-g^+-tttt)_n$ could be expected to be energetically acceptable. Similar considerations apply to the $(-g^+t-tttt-g^-t-tttt)_n$ sequence and it should be easily apparent that these conformations are of the glide type. The latter sequence is indeed acceptable and brings to a fiber repeat of 12.2 Å containing 2 monomer units with an energy of 0.9 kJ/mole above the minimum, just like the 3_1 helical conformation. On the contrary the $(-g^+g^+-tttt-g^-g^+-tttt)_n$ conformation leads to ring closure after four monomer units and must be discarded. The small energy differences among the different acceptable conformers should be further reduced in the crystal since the structures that have higher energy are more extended and are likely to pack more efficiently. The present result clearly suggests an all *trans* conformation for the melt spun fiber data (form III). With respect to the other crystalline modifications it is premature to attempt definite conformational assignments. The calculations are consistent however with the experimental observation of a number of different crystalline polymorphs as a result of the accessibility of a variety of regular, low energy conformational states.

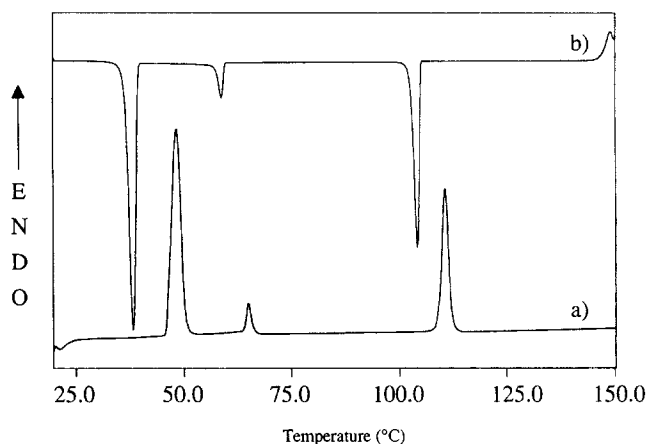


Figure 9 DSC curves for the DTC monomer: (a) heating scan; (b) cooling

The arguments applied to periodical conformations can be extended to irregular sequences like $g^+t-tttt-g^-g^--tttt-tg^+-tttt-tg^-tttt$. In fact any combination of successive acceptable $\gamma\gamma'$ torsion angle pairs, namely g^-g^- , g^+g^+ , tg^- , tg^+ , g^-t , g^+t and tt is in principle energetically viable. This obviously does not imply that any sequence of successive acceptable $\gamma\gamma'$ pairs will be feasible in a crystalline or even in a mesomorphic architecture. However loose, cooperative disordering of successive $\gamma\gamma'$ pairs may reasonably affect only local order leaving the macromolecules largely parallel to the original direction in an extended, low energy conformation, especially if kink-forming (g^-g^-) and (g^+g^+) are avoided. The model we propose is broadly related to the type of conformational disorder discussed by Corradini¹⁵ in the case of poly(1,4-*trans*-butadiene) and poly(1,4-*cis*-isoprene). The availability of various low energy conformers preserving chain extension and directionality represents indeed the prerequisite¹⁰ for the development of conformational disordered crystals. This reasoning may well justify the occurrence of the mesomorphic form II, discussed in the previous section.

Crystallographic and thermal characterisation of DTC

Figure 9 shows the DSC curves recorded between 0°C and 150°C at 20°C/min and in Table 3 thermal data for the cyclic monomer (DTC) are reported. Consistent with

Table 3 Thermal behavior of DTC

	T1 (°C)	ΔH1 (J/g)	T2 (°C)	ΔH2 (J/g)	T3 (°C)	ΔH3 (J/g)
First Heating	50	58	66	6	112	36
Cooling	41	−64	61	−5	106	−32
Second Heating	49	64	66	5	111	39

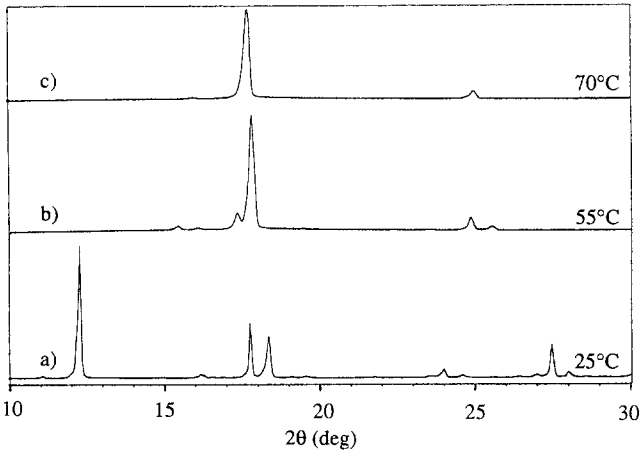


Figure 10 X-ray diffraction patterns of DTC recorded at different temperatures on heating: (a) 25°C (form I); (b) 50°C (form II); and (c) 70°C (form III)

literature data,⁹ in the first and in subsequent heating cycles three endotherms respectively at 50°C, 66.5°C and 112.0°C are apparent and in cooling scans the three corresponding exothermic peaks result. Figure 10 shows X-ray diffraction patterns of DTC powder samples (10 < 2θ < 30) recorded at different temperatures: namely 25°C (a), 55°C (b) and 70°C (c). The data evidence the polymorphic nature of DTC, characterised by three different crystalline modifications, which will be referred to respectively as form I (below 50°C), form II (between 50 and 65°C), and form III (between 66°C and the isotropisation).

Dilatometric results (Figure 11) in agreement with DSC data also show three transitions respectively at 47°C (from 0.810 to 0.875 cm³/g), at 62°C (from 0.875 to 0.885 cm³/g)

and at 112°C (from 0.910 to 0.940 cm³/g). The values of specific volume and enthalpy changes for the different transitions correlate well: melting of form I, for example, involves both substantial V_{sp} and enthalpy changes.

The molecular structure of the low temperature form I of DTC is shown in Figure 12. The two independent molecules in the asymmetric unit (Figure 13) display very similar geometries and molecular dimensions (Table 4) are closely comparable to the envelope model obtained by conformational energy calculations in which C1, O2, O3, C2 and C4 are nearly coplanar. Indeed this is the only acceptable energy minimum. Conformational calculations carried out with the MM2 force field also show that the envelope can flip, through a path involving twist-boat conformations, with a barrier of about 20 kJ/mole between the two enantiomorphous equivalent envelope conformers, both of which are characterised by a symmetry plane through atoms O1, C1, C3, C5 and C6. In form I crystals we have no evidence of disorder of this kind and in fact even the mentioned intramolecular symmetry is lost probably due to packing effects. Small but significant differences occur between the torsion angles C1–O2–C2–C3 (−35° and −38° for the two independent molecules A and B respectively) and C1–O3–C4–C3 (28° and 25° for A and B).

Lebedev *et al.*⁹ because of the high temperature and the low melting entropy of form III suggest that both form II and form III are plastic crystal mesophases, resulting from orientational disordering of molecules in the crystal lattice. It is also suggested that the transition around 60°C is associated with conformational disorder affecting the ring geometry. Plastic crystals, however, as a result of orientational disorder and of high mobility, present diffraction patterns with only few reflections, which can be usually indexed in the cubic system (normally body or face centred) as one would expect for crystals motifs of

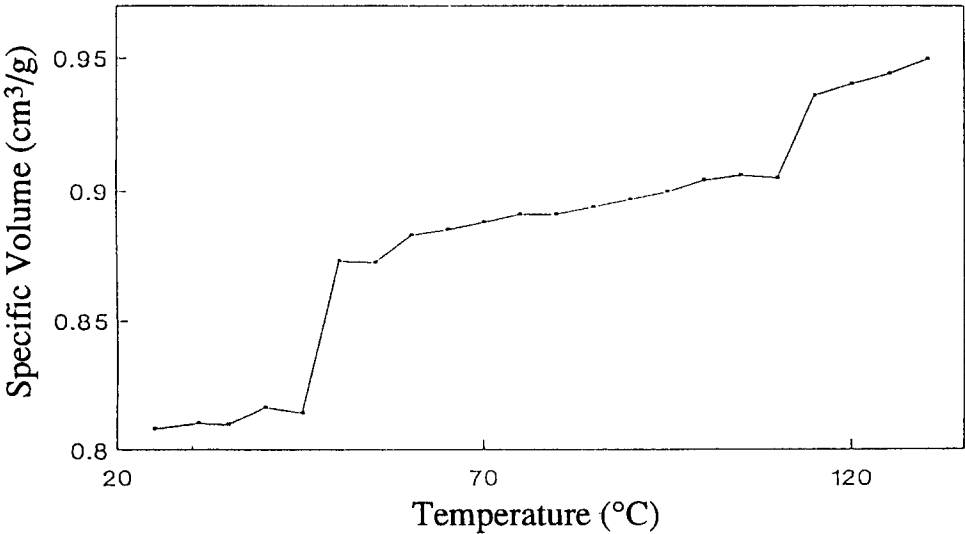
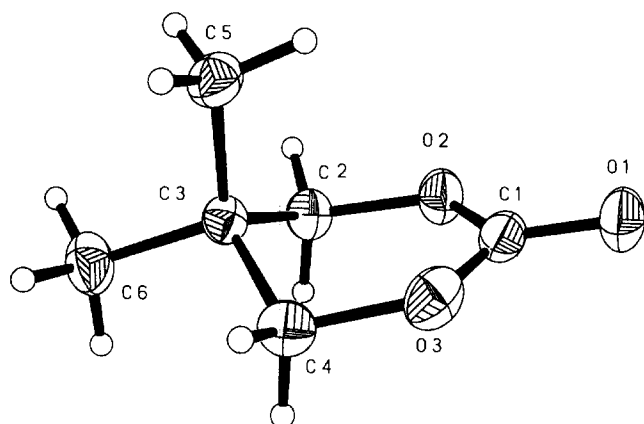


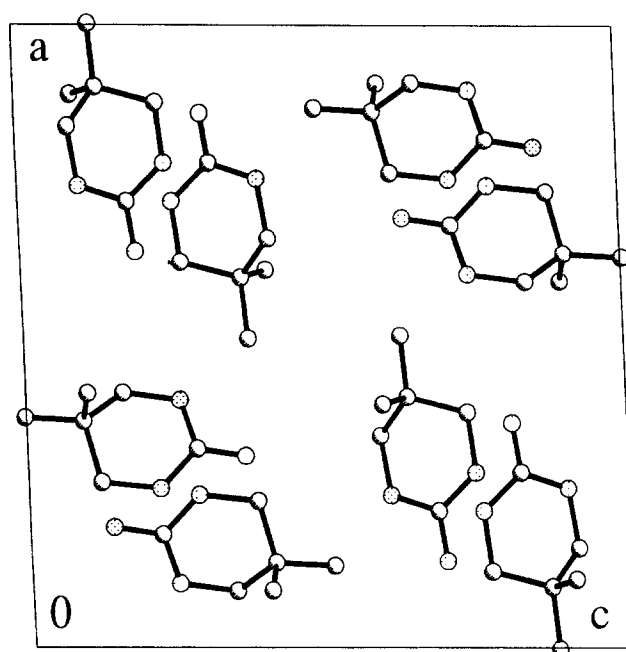
Figure 11 Dilatometric curve of DTC

Table 4 Geometrical features^a of DTC form I

	Molecule A	Molecule B
<i>Bond lengths (Å)</i>		
O1–C1	1.198 (3)	1.197 (2)
O2–C1	1.313 (3)	1.328 (3)
O2–C2	1.449 (2)	1.443 (3)
O3–C1	1.317 (3)	1.311 (3)
O3–C4	1.451 (3)	1.445 (2)
C2–C3	1.496 (3)	1.500 (3)
C3–C4	1.495 (3)	1.501 (3)
C3–C5	1.521 (3)	1.514 (3)
C3–C6	1.525 (3)	1.526 (3)
<i>Bond angles (deg)</i>		
C1–O2–C2	122.3 (2)	120.5 (2)
C1–O3–C4	121.1 (2)	123.1 (2)
O1–C1–O2	120.2 (2)	120.7 (2)
O1–C1–O3	119.4 (2)	119.5 (2)
O2–C1–O3	120.4 (2)	119.8 (2)
O2–C2–C3	112.2 (2)	111.6 (2)
C4–C3–C2	105.5 (2)	105.0 (2)
C4–C3–C5	111.0 (2)	109.8 (2)
C2–C3–C5	111.5 (2)	109.5 (2)
C4–C3–C6	109.3 (2)	111.2 (2)
C2–C3–C6	109.6 (2)	110.8 (2)
C5–C3–C6	110.0 (2)	110.3 (2)
O3–C4–C3	111.6 (2)	112.8 (2)
<i>Torsion angles (deg)</i>		
C4–O3–C1–O1	179.5 (2)	179.0 (2)
C4–O3–C1–O2	– 2.3 (3)	– 2.1 (3)
C2–O2–C1–O1	– 176.1 (2)	– 172.2 (2)
C2–O2–C1–O3	5.8 (3)	8.9 (3)
C1–O2–C2–C3	– 34.6 (3)	– 38.5 (3)
O2–C2–C3–C4	55.4 (2)	56.6 (2)
O2–C2–C3–C5	– 65.4 (2)	– 63.4 (2)
O2–C2–C3–C6	173.2 (2)	174.2 (2)
C1–O3–C4–C3	28.0 (3)	25.5 (3)
C2–C3–C4–O3	– 52.3 (2)	– 50.3 (2)
C5–C3–C4–O3	68.2 (2)	69.9 (2)
C6–C3–C4–O3	– 169.8 (2)	– 168.1 (2)

^aEstimated standard errors in parentheses.

Figure 12 ORTEP view of one of the two visually non-distinguishable independent DTC molecules in form I crystals

spherical shape. Furthermore plastic crystals are not birefringent because of the nearly isotropic nature of the high symmetry cubic crystals. Judging from the diffraction data at 55°C, where form II is stable, it appears unlikely that form II is a plastic crystal phase because the many observed reflections cannot be indexed in the cubic system. Furthermore optical microscopy data at 55°C indicate a residual birefringence. The 50°C phase transition could therefore arise from the conformational motions involved in


Figure 13 Projection in the (a,c) plane of the packing of form I DTC

the flipping between the two envelope conformers of the six membered ring. This idea is suggested also by the crystal structure of the closely related perhydropyrimidin-2-one molecule¹⁶, which presents disorder on two positions for the apical atom in the envelope [i.e. C(3) in Figure 12]. The large change in enthalpy and specific volume for the 50°C transition of DTC may relate to the substantial disruption of the lattice caused by the flipping motions. A tentative cell with $a = 7.12$, $b = 10.40$, $c = 10.09$ Å, $\beta = 86.5^\circ$ indexes the observed diffraction maxima of form II with $Z = 4$ and a volume per monomeric unit only slightly smaller than the value of 189 Å^3 determined from dilatometric measurements.

At 70°C the X-ray diffraction patterns show substantially fewer reflections and the birefringence is lost completely. These facts indicate that form III could be a plastic crystalline phase of anisotropic molecules. The low volume change, instead of the large one normally leading to cubic plastic crystals may result from uncomplete orientational averaging (e.g. around one axis) of the still anisotropic, already conformationally disordered molecules. The reflections of form III are indexable with a tetragonal cell with $a = b = 11.35$ and $c = 5.87$ (Z = 4) in close agreement with a dilatometric volume of 192 Å^3 per monomeric unit.

CONCLUDING REMARKS

Diffraction and thermal studies show that PDTC is able to crystallise in at least three different forms which are likely to adopt different conformations. This is in agreement with conformational calculations indicating four extended low energy regular conformations within less than 3.5 kJ/mole. In addition a large number of different irregular conformations leaving the polymer molecule extended are accessible, allowing us to envisage the possibility of conformationally disordered crystalline modifications. Indeed a number of experimental features suggest that the high temperature form II is a higher entropy modification than the solution crystallised form I, namely: (1) the lower melting enthalpy;

(2) the higher melting temperature; (3) the very small recrystallisation undercooling; (4) the exceptionally large form II coherent domain dimensions; (5) the chain extended morphology. We can thus suppose that form II is, at least in the incipient crystallisation stages, a conformationally disordered phase, mesomorphic in nature. It is interesting to note that while for relatively high molecular weight PDTC7 mesomorphic samples appear to have at least a kinetic stability, lower molecular weight PDTC2 samples show a tendency to develop further order upon cooling below 100°C.

The conformational disorder invoked to account for the behaviour of the polymer is also supported by the polymorphic behaviour of the DTC monomer showing two high temperature modifications characterised by high entropy. Analysis of the crystal structure of DTC and of related compounds suggests the possibility of conformational disorder also in the monomer. Further work is in progress to characterise the detailed molecular organisation in the different polymorphs of DTC, PDTC and its copolymers.

ACKNOWLEDGEMENTS

This research has been partly supported by the Italian Ministero dell'Università e della Ricerca Scientifica (MURST, 40%) and Consiglio Nazionale delle Ricerche, progetto strategico tecnologie chimiche innovative. Encouraging discussions with Professor G. Allegra are acknowledged.

REFERENCES

1. Klee, D., Schmidt, P., Beyss, E., Kleiker, H., Mittermayer, C. and Höcker, H., *Adv. Biomaterials*, 1992, **10**, 431.
2. Keul, H., Bächer, R. and Höcker, H., *Makromol. Chem.*, 1986, **187**, 2579.
3. Wurm, B., Keul, H. and Höcker, H., *Macromol. Chem. Phys.*, 1994, **195**, 3489.
4. Altomare, A., Casarano, G., Giacovazzo, C. and Guagliardi, A., *J. Appl. Cryst.*, 1993, **26**, 343.
5. Sheldrick, G. M., *SHELXL93, Program for the Refinement of Crystal Structures*, Univ. of Göttingen, Germany, 1993.
6. Dauber-Osguthrope, P., Roberts, V. A., Osguthrope, D. J., Wolff, J., Genest, M. and Thagler, A., *Proteins: Struct. Funct. Genet.*, 1988, **4**, 31.
7. *Dynamics Calculation from Discover and Graphical Display Using Insight II Version 2.3.0*, Biosym Technologies, San Diego, 1994.
8. *Macromodel-Interactive Molecular Model System—Version 4.0*, Columbia University, New York, 1993.
9. Lebedev, B. V., Kulagina, T. G., Telnoy, V. I. and Vasil'ev, V. G., *Macromol. Chem. Phys.*, 1995, **196**, 3487.
10. Wunderlich, B., Möller, M., Grebowicz, J. and Baur, H., *Adv. in Polymer Science*, 1987, **87**, 1.
11. Ferro, D. R., Brückner, S., Meille, S. V. and Ragazzi, M., *Macromolecules*, 1990, **23**, 1676.
12. Brückner, S., Meille, S. V., Malpezzi, L., Cesàro, A., Navarini, L. and Tombolini, R., *Macromolecules*, 1988, **21**, 967.
13. Perez, S. and Scaringe, R. P., *Macromolecules*, 1987, **20**, 68.
14. Corradini, P., *The Stereochemistry of Macromolecules*, ed. A. D. Ketley, Vol. 3, Marcel Dekker, New York, 1968.
15. Corradini, P., *J. Polym. Sci. Polym. Symp.*, 1975, **50**, 327.
16. Calogero, S., Russo, U. and Del Prà, A., *J. Chem. Soc. Dalton Trans.*, 1980, 652.